



OPEN

Two Quenchers Formed During Photodamage of Photosystem II and The Role of One Quencher in Preemptive Photoprotection

Alonso Zavafer ^{1,6*}, Ievgeniia Iermak^{2,3,4,6}, Mun Hon Cheah ^{1,5} & Wah Soon Chow¹

The quenching of chlorophyll fluorescence caused by photodamage of Photosystem II (qI) is a well recognized phenomenon, where the nature and physiological role of which are still debatable. Paradoxically, photodamage to the reaction centre of Photosystem II is supposed to be alleviated by excitation quenching mechanisms which manifest as fluorescence quenchers. Here we investigated the time course of PSII photodamage *in vivo* and *in vitro* and that of picosecond time-resolved chlorophyll fluorescence (quencher formation). Two long-lived fluorescence quenching processes during photodamage were observed and were formed at different speeds. The slow-developing quenching process exhibited a time course similar to that of the accumulation of photodamaged PSII, while the fast-developing process took place faster than the light-induced PSII damage. We attribute the slow process to the accumulation of photodamaged PSII and the fast process to an independent quenching mechanism that precedes PSII photodamage and that alleviates the inactivation of the PSII reaction centre.

Photosynthesis is the biochemical reaction that sustains most ecosystems on Earth. However, this process has an intrinsic suicidal nature, as the light absorbed by the photosynthetic machinery leads to chemical modifications (photodamage) causing its inactivation (photoinactivation)¹. Among all the components of photosynthesis, photosystem II (PSII) is most vulnerable to photodamage². Two types of photoinactivation can be identified^{3,4}. Total PSII and PSII reaction centre (RC) photoinactivation. Total PSII photoinactivation refers to light-induced loss of the oxygen evolution (a process that requires an active Mn₄CaO₅ cluster and an active RC). On the other hand, RC photoinactivation involves inhibition of the capacity of RC to reduce Q_A, the primary quinone acceptor of electrons. While there is no consensus about the causes, primary site(s) and molecular mechanism of total PSII photodamage^{1,5}, it is accepted that RC photodamage is mostly dependent on excitation pressure and driven by pigment absorption.

Based on photosensitisers, two hypotheses have been proposed to explain total PSII photodamage. The *light energy absorption by photosynthetic pigments model* proposes that photodamage is caused by excessive photon absorption or/and charge recombination reactions^{5–11}. By contrast, the *Mn photoinactivation model* suggests that photodamage of PSII is caused by direct absorption of light by the Mn₄CaO₅ cluster^{3,12} within PSII and is independent of excessive excitation of chlorophyll.

It is widely accepted that PSII photodamage is alleviated by protection mechanisms, collectively termed photoprotection¹³. As the main cause of photodamage has been considered to be excessive absorption of energy, non-photochemical quenching (NPQ), has been proposed as a way to dissipate the excessive excitation that can otherwise induce PSII photodamage^{13,14}. For supporters of the Mn photoinactivation model, the physiological role of NPQ is not to avoid Total PSII damage but to protect RC and the PSII repair mechanisms¹⁵. Even though most reports about NPQ acknowledge its role as a mechanism of Total PSII photoprotection^{13,14,16–18}, experimental

¹Research School of Biology, College of Science, The Australian National University, Canberra, ACT, 2601, Australia.

²Laboratory of Biophysics, Wageningen University, P.O. Box 8128, 6700, ET, Wageningen, The Netherlands.

³BioSolar Cells Project Office, P.O. Box 98, 6700, AB, Wageningen, The Netherlands. ⁴Present address: São Carlos Institute of Physics, University of São Paulo, São Carlos, SP, Brazil. ⁵Present address: Department of Chemistry, Uppsala University, Uppsala, Sweden. ⁶These authors contributed equally: Alonso Zavafer and Ievgeniia Iermak.

*email: alonso.zavaleta@anu.edu.au

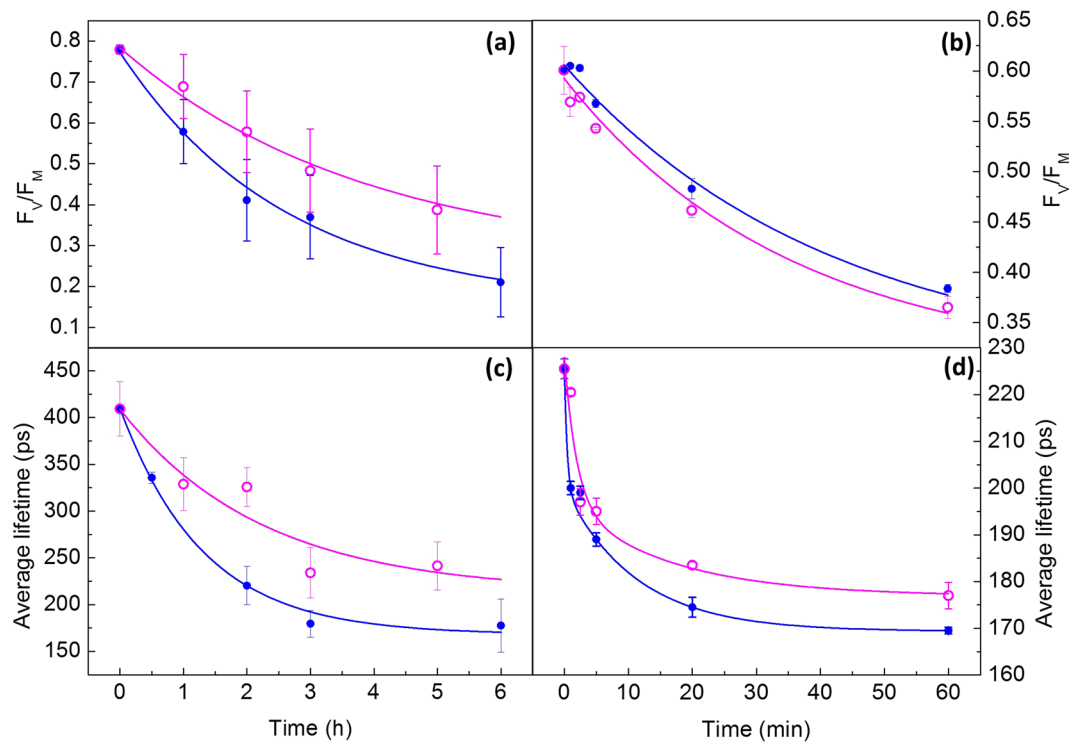


Figure 1. Changes in PSII efficiency and average fluorescence lifetimes after illumination with 460 nm (blue data points) and 660 nm (purple data points) light. Effect of photodamage on PSII efficiency (F_v/F_M) in (a) spinach leaves, (b) BBY's. Changes in average fluorescence lifetimes upon illumination, measured on (c) spinach leaves, (d) BBY's. Fitting results using Eqs 2 and 3 (see Supplementary Materials and Methods) are represented by continuous lines. Average values for F_v/F_M or average fluorescence lifetimes are presented \pm standard deviation. Each point represents $n = 5$ (with the exception of panel (b) which corresponds to $n = 10$). The experiment was replicated twice; data presented corresponds to one replicate. Fitting parameters and statistical analysis are included in Supplementary Material.

evidence suggests that quenching of excitation has low efficiency in protecting against the light-induced loss of the Total PSII activity^{15,19–21}. Thorough studies that analyse the relationship between NPQ and photoprotection have been reported²², but most studies do not take into consideration either wavelength dependence of photodamage or inhibition of PSII repair.

One of the consequences of PSII inactivation is fluorescence quenching. This type of quenching, termed qI, has been attributed to several causes and primarily to long-lasting qE and qZ mechanisms (such as Δ pH, xanthophylls, etc). However, it was demonstrated, by measuring chlorophyll fluorescence lifetime, that even in the absence of NPQ mechanisms (particularly qE and qZ) quenching still occurs²³. The origin and physiological role of qI mechanisms remain unknown.

In order to gain further insights into the qI, we investigated the time course of the decrease of average fluorescence lifetime (τ_{AV}) to scrutinize its role in photodamage. To see if the decrease of τ_{AV} only occurs in leaves or is intrinsic to PSII, changes in τ_{AV} were evaluated during the time course of PSII photodamage *in vitro*. Two experimental model systems under the excessive excitation were compared: photorepair-impaired spinach leaves (*in vivo* system) and PSII enriched membranes (here on referred to as BBY's, an *in vitro* system). Since the decrease in τ_{AV} might be related to damage of the Mn_4CaO_5 cluster or induced by photosynthetic pigments, we compared the effect of blue light (where more damage to Mn_4CaO_5 cluster has been observed) versus red light where photodamage is mostly driven by photosynthetic pigments. The time-dependent PSII activity decrease and quenching fluorescence lifetime are compared to the time course of PSII photoinactivation.

Results

PSII photodamage is accompanied by shortening of τ_{AV} . To test if photodamage (*in vivo* and *in vitro*) occurs in parallel with the shortening of τ_{AV} , the time courses of the decrease in the maximum efficiency for primary photochemistry of PSII (F_v/F_M) and in the fluorescence lifetime were measured. F_v/F_M corresponds to the ratio of variable to maximum chlorophyll fluorescence. It is known²⁴ that a decrease in the maximum efficiency for primary photochemistry of PSII, measured as F_v/F_M , reflects the magnitude of PSII photodamage if repair is absent. Both experimental model systems were illuminated with $1300 \mu\text{mol photons m}^{-2} \text{s}^{-1}$. Figure 1a,b show that for both illumination wavelengths and samples, 460 and 660 nm, the F_v/F_M decreased with time. The decrease in the photochemical efficiency was fitted using Eq. 2 (see Supplementary Information) and the fit parameters are presented in Table 1 (and Supplementary Figs 1 and 2). Figure 1a,c show the data obtained for illuminated leaves. Both data sets were fitted to a single exponential decay (with rate coefficient k_{PI} and a residual term), whereas

	λ (nm)	T_{50} (F_V/F_M)	Ratio $\frac{660}{460}$	T_{50} (τ_{AV})	Ratio $\frac{660}{460}$
*Leaves	460	1.8 \pm 0.3 (0.6)	1.81	0.9 \pm 0.2 (242)	1.72
	660	3.3 \pm 1.0 (0.6)		1.55 \pm 0.6 (197)	
**PSII-enriched membranes	460	28.8 \pm 5.5 (0.5)	0.85	4.5 \pm 0.6 (49)	1.09
	660	24.7 \pm 5.5 (0.5)		4.9 \pm 0.4 (56)	

Table 1. Values of half-lifetime (T_{50}) obtained for decreases in PSII efficiency (F_V/F_M) and τ_{AV} for 460 and 660 nm illumination in leaves and BBY's. T_{50} values are presented \pm standard error and amplitudes are presented in parenthesis. The first ratio 660/460 reflects the ratio of T_{50} values obtained for F_V/F_M at 660 and 460 nm. The second ratio 660/460 reflects the ratio of T_{50} values obtained for τ_{AV} at 660 and 460 nm. *Units in hours for T_{50} . **Units in minutes for T_{50} .

changes in the τ_{AV} in Panel c were fitted to a double exponential. The criteria to fit each signal were based on using the best fitting for the obtained results.

In order to facilitate a comparison between different treatments, the time point where 50% of the changes were observed ($T_{50} = \ln 2/k_{PI}$) were compared for both experimental model systems. It was observed for illuminated leaves that for 460 nm illumination, T_{50} is smaller than for 660 nm (see Table 1). These data are in good agreement with the previously reported action spectra of photodamage for different species^{3,12,21,25} where the blue region of the visible spectrum induced more damage than the red region. By contrast in leaves the decay of F_V/F_M for both wavelengths was the same in BBY's (see Table 1).

Photodamage was accompanied by shortening of τ_{AV} in both leaves and BBY's, as presented in Fig. 1c,d. In the case of leaves (Fig. 1c) illumination with 460 nm light induced a faster shortening of τ_{AV} than illumination with 660 nm light. This shortening of τ_{AV} can be described by a double-exponential decay and the fitting parameters are presented in Table 1 (and Supplementary Table 2).

BBY's do not show a statistically significant difference in τ_{AV} for 460 nm and 660 nm light (Table 1). The observed time course does not follow a simple first-order rate law; at least two components are needed (Eq. 3, see Supplementary Information). This can be interpreted as two quenching processes occurring in BBY's. It is remarkable that for both wavelengths most of the changes in τ_{AV} occur during the first minutes of illumination.

It has been hypothesized that PSII photodamage increases the yield of fluorescence in the F_O state^{24,26}. An increase of F_O corresponds to an increase of the average fluorescence lifetime of PSII. However, it was reported²³ that even in the absence of NPQ, τ_{AV} decreased with illumination time when measured in the F_M state (closed PSII RCs). In the dark-adapted state, as measured in present study, the τ_{AV} is expected to be shortest under control conditions since all RCs are expected to be open. Energy cannot be used more efficiently by the RCs than in the dark adapted state. Therefore, the observed shortening of τ_{AV} must be interpreted as an energy dissipation event which is different from primary photochemistry. It is worth noting that under control conditions (darkness across the time course) no significant changes in τ_{AV} and F_V/F_M were observed *in vivo* or *in vitro* (Supplementary Fig. 2).

In Supplementary Fig. 3 (shifting of histograms) and 4 (representative micrographs) the changes in τ_{AV} of leaves after 460 and 660 nm illumination are shown and the values of τ_{AV} are colour coded. The various images taken at different time points show that τ_{AV} shortens during the illumination experiment for both illumination wavelengths. We observed that a change in τ_{AV} occurred in the whole chloroplast and that there was heterogeneity among chloroplasts within the same focal plane.

The decrease in average fluorescence lifetime is faster than the increase in PSII photodamage.

If the changes in τ_{AV} are a consequence of photodamage that leads to the decrease of F_V/F_M , they should occur at an equal or lower rate as changes in PSII efficiency. Which is not what is observed in the present experimental observation.

Table 1 shows that τ_{AV} in leaves (0.9 h at 460 nm and 1.6 h at 660 nm) decreased faster than PSII efficiency (1.8 h at 460 nm and 3.3 h at 660 nm) for both wavelengths (T_{50} for decrease in τ_{AV} is 2 times smaller than the T_{50} for photodamage, see Table 1). This implies that the decrease in τ_{AV} cannot be solely explained by loss of maximum PSII efficiency. Similarly, BBY's showed a faster decrease in τ_{AV} (4.5 min at 460 nm and 4.9 min at 660 nm) than PSII efficiency ($\Sigma 28$ min for both wavelengths); $T_{50}(\tau_{AV})$ is 3.4 times smaller than $T_{50}(F_V/F_M)$ in the case of 460 nm excitation, while for 660 nm it is 6.1 times smaller. Despite the differences in complexity between *in vivo* and *in vitro* (BBY's do not have an unlimited source of electron acceptors, PSI is absent, and other molecular pathways are not present), both experimental model systems showed: (1) photodamage shows single exponential behaviour; (2) higher rate of photodamage induced by 460 nm than by 660 nm light; (3) shortening of τ_{AV} ; (4) a faster decrease of τ_{AV} than of PSII efficiency. All these observations support the idea that the mechanism(s) of photodamage and quenching *in vitro* and *in vivo* have a common origin.

Analysis of the fluorescence lifetime components and populations shows that there are at least two types of quenchers formed, one dependent on and one independent of photodamage.

In leaves, decrease in τ_{AV} can be satisfactorily fitted with a single exponential, so only one population of quenched PSII was observed. However, it is possible to analyse the three individual lifetime components of the τ_{AV} (each lifetime component, $a_i \cdot \tau_{PI}$, has its own amplitude and lifetime) to establish the relative contributions of individual quenching events to the overall decrease in τ_{AV} . It is possible to discern the presence of either one or several quenchers by comparison between the three individual lifetime components of τ_{AV} to T_{50} of loss of F_V/F_M

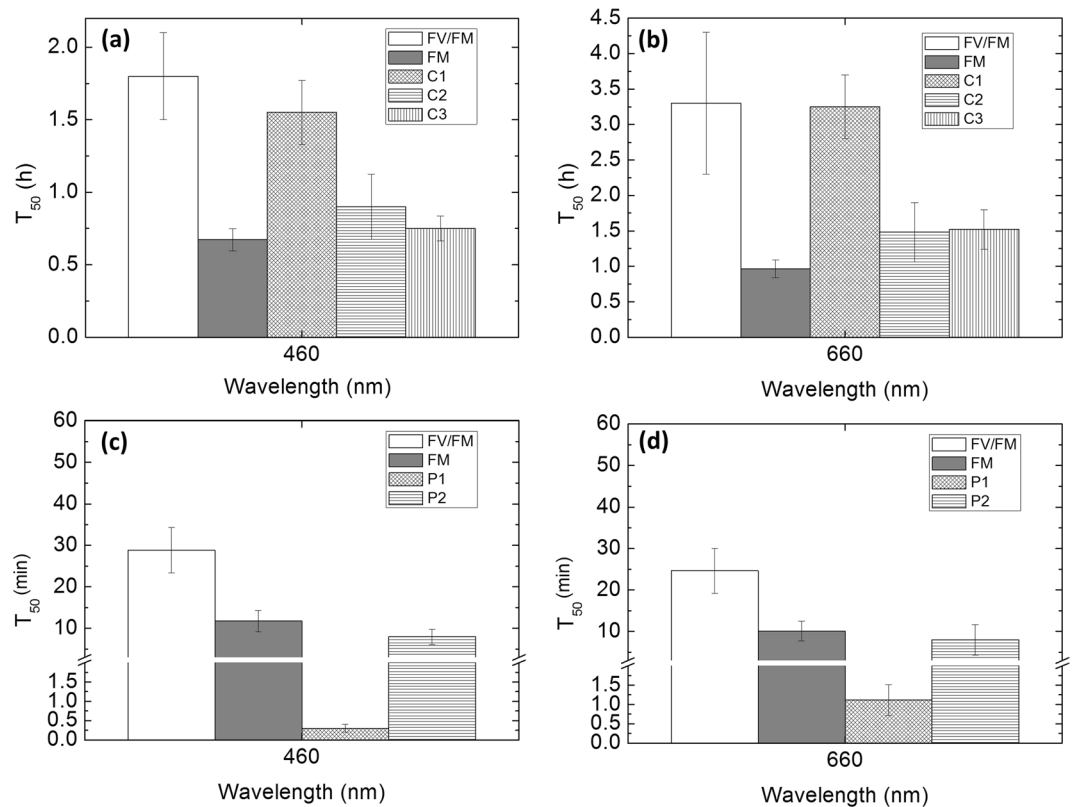


Figure 2. Values of half-time (T_{50}) obtained for changes in the individual decay components ($a_i \cdot \tau_i$) of fluorescence τ_{AV} of leaves for 460 Panel (a) and 660 Panel (b) nm illumination, and formation of two populations of quenched PSII's in BBY's Panel (c) for 460 nm and Panel (d) for 660 nm, compared to the T_{50} values of F_V/F_M and F_M . T_{50} values are presented with standard error. Each point represents $n = 5$ (with the exception of the F_V/F_M of BBY's which corresponds to $n = 10$). The experiment was replicated twice, and data presented corresponds to one replicate. Fitting parameters and statistical analysis are included in Supplementary Material.

(Fig. 2a,b). It was observed that the first component ($C1 = a_1 \cdot \tau_1$, which had the shortest fluorescence lifetime) has a T_{50} value similar to that of the loss of F_V/F_M for both illumination wavelengths. The second component of the fluorescence lifetime ($C2$) had shorter T_{50} values (faster development) than that of photodamage but similar to the T_{50} of the decrease of F_M at both wavelengths. The T_{50} of the third component ($C3$) was statistically similar to that of F_M decrease for 460 nm but that was not the case at 660 nm. This suggests that there are at least two distinct quenching processes occurring in parallel in leaves, one where the quencher is formed as a result of photodamage and another where the quencher (represented by $C2$) is dependent only on illumination. The latter was formed faster and explains why the change in τ_{AV} has shorter T_{50} values than the T_{50} of the loss of F_V/F_M . It is worth noting that the decrease of F_O was very slow and cannot be satisfactorily fitted appropriately to our single exponential model (See Supplementary Fig. 5).

In *in vitro* measurements, decrease in τ_{AV} can be satisfactorily fitted as double exponential indicating two populations of quenched PSII being formed in response to illumination (decrease of τ_{AV}). The first (fast) population was quenched almost immediately after illumination started (0.3 and 1.1 min for 460 and 660 nm respectively) and the second population formed in a slower manner (approximately 8 min). The decay in F_O was remarkably faster and it was not possible to fit the data points in a satisfactory manner (see Supplementary Fig. 5). By contrast, the T_{50} for the changes in F_M is statistically similar to the T_{50} of the slow population. None of the two quenched populations seemed to correspond to photodamaged PSII as none of them matched the T_{50} of decrease of PSII maximum efficiency. The analysis of individual components of BBY's was not possible as each component followed a complex kinetics that did not adjust to first or second order rate laws and for this reason were not taken into account for interpretation.

Photodamage to the RC is slower than Total PSII inactivation and dependent on excessive pigment excitation. Three independent reports^(3,4,12) have shown that RC photoinactivation is slower than Total PSII inactivation. Also, it was shown that RC inactivation is dependent on excessive pigment excitation. We have shown that quenchers can be formed before Total PSII inactivation takes place, so it is within reason to hypothesize that the observed quenchers photoprotect the RC to some extent. For this reason, we have estimated the effect on the electron transport rate (ETR) activity of PSII at the time point corresponding to T_{50} of photodamage (which was estimated by PSII efficiency).

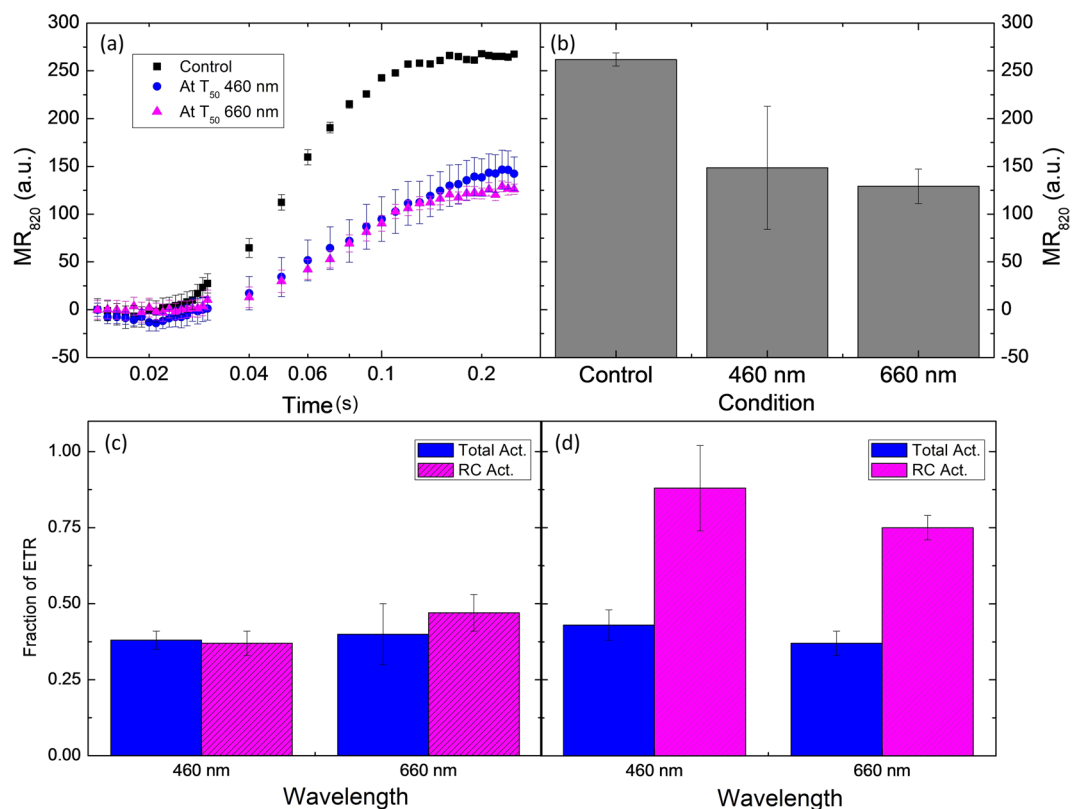


Figure 3. Panel (a): modulated reflectance changes at 820 nm of P700 in leaves for control and both illumination wavelengths (460 and 660 nm) at the T_{50} time point. Panel (b) displays the net amplitude of the P700 accumulation at 220 ms for control and both illumination wavelengths (460 and 660 nm). In panel (c,d) the fraction of ETR of BBY's is shown the corresponding value of T_{50} of photodamage (min) of illumination. ETR was estimated through absorption changes of DCPIP at 600 nm. Total PSII activity (act.) was calculated from H_2O to DCPIP and reaction centre (RC) activity (act.) was calculated from DPC to DCPIP. Panel (c), an experiment with no chemicals added during photodamage experiments (control). In panel (d), PPBQ (300 μM) and DPC (300 μM) were present during photodamage experiments. Each point represents $n = 5$; the experiment was replicated three times, and data presented corresponds to one replicate. T-test was performed between Total PSII activity vs. RC activity, significant difference is denoted by * at a $p > 0.05$.

Due to the difference between *in vivo* and *in vitro* two approaches were used to estimate the effect on ETR. For leaves the relative ETR was estimated using the modulated reflectance changes at 820 nm of P700 by measuring the amplitude between 0.014 s to the maximum reflectance intensity usually located around 0.2 s (during illumination). In Fig. 3a, a comparison between the efficiency to pump electrons from PSII to PSI (re-reduction of $P700^+$) is presented for both wavelengths at the T_{50} time point (2 h for 460 nm and 3 h for 660 nm). As expected from the F_V/F_M kinetics, at T_{50} of both conditions PSII activity dropped by the same magnitude, indicating that the electron flow between both systems (ETR) was impaired. Figure 3b displays the net amplitude of the P700 accumulation at 220 ms (maximum P700 value for the control), for 460 nm a decrease in the activity of $\Sigma 60\%$ was observed while for 660 nm the decrease was $\Sigma 50\%$. One should note that the difference between illuminations is not statistically significant, but both are statistically different from the control condition. This confirms that PSII of illuminated leaves were indeed photoinactivated.

In order to estimate ETR *in vitro* a colorimetric DCPIP assay was used (Fig. 3c,d). This method allows the two activities to be probed separately (total PSII activity and RC activity, see methods). Photodamaged samples illuminated in the absence of electron acceptors showed that RC inactivation was significantly lower than the loss of total activity ($t\text{-test}_{460nm} < 0.1$ and $t\text{-test}_{660nm} < 0.05$) at T_{50} . This effect was observed to a greater extent if the sample was exposed under the presence of artificial electron donor (DPC) and acceptor (PPBQ), where RC inactivation was only approx. 20% and significantly lower ($t\text{-test} < 0.001$ at both wavelengths). This indicates that RC damage is clearly dependent on excitation pressure and slower than total PSII inactivation.

Comparison of the ETR measurements and PSII efficiency for dark controls and photodamage are presented in Supplementary Fig. 6.

Discussion

In this work, we address the issue that photodamage is accompanied by a decrease in τ_{AV} in two experimental model systems under excessive excitation. We will analyse four possible scenarios that can explain the observed quenching due to PSII photodamage and shortening of τ_{AV} :

- (1) Quenching represents the first alterations in the PSII functionality (there is no photoprotective effect)^{27,28};
- (2) Long lasting qE, qZ, and qT^{29–32};
- (3) Dissipation of excessive light energy from active PSII by neighboring inactivated PSII RCs^{23,33}, implying that photodamaged PSII centres have a photoprotective role²³;
- (4) Accumulation of a photoproduct, not related to photodamaged PSII itself³⁴.

Scenario 1 would imply that the observed quenching effect is a direct consequence of photodamage that inactivates PSII. Here, we demonstrate that the overall quenching in the two model systems occurred faster than the accumulation of PSII photodamage. It has been hypothesized that PSII photodamage should increase the yield of fluorescence in the F_O state²⁶, but this should be manifested as an increase of τ_{AV} which is contrary to experimental observations in both model systems.

Scenario 2 would link some components of qI with residual of qE, qZ, and qT mechanisms. One possible explanation of the long lasting quenching is a manifestation of qI at the antenna³⁵, and the decrease of F_V/F_M is due to long lasting qZ. In both *in vivo* and *in vitro* models, F_M decreased faster than F_V/F_M . *In vivo* the quencher that is accumulated faster seems to be correlated with F_M which in turn reflects the changes in the efficiency of energy dissipation³⁵. However, this process should not occur *in vitro*, where the decrease in F_M is also faster than F_V/F_M . For this reason, component 2 cannot be directly related to a long lasting qZ mechanism.

Also, it has been reported that a non-linear relationship of photoprotection and quenching is possible²². However, in this work samples were measured several hours after photodamage, indicating that the observed quenching is a long-lived component of qI. It was demonstrated²³ that quenching during photodamage occurs regardless of the use of DTT and nigericin in leaves which discards the role of qE, qZ, and qT as the sole explanation of the observed quencher. The alternative is that dark-sustained xanthophyll would be accumulated, but this type of quenching has τ_{AV} longer than F_O ³⁶, which is contrary to present observations. Furthermore^{37,38}, demonstrated that violaxanthin conversion occurs very slowly in leaves not acclimated to chilling temperatures, as in the present study, so the contributions of qZ in this particular case would not explain alone the strong quenching effect. Finally, these types of quenching are not present in BBY's.

Scenario 3 attributes the origin of the quencher to inactive photodamaged RCs³³, that concomitantly protect neighbouring active PSII by dissipating excessive excitation. This scenario is dependent on PSII photodamage, as the quenchers are the inactivated PSII. In leaves, a direct relation between photoinactivated PSII and formation of quenchers could be established because of the similarities of T_{50} of decrease in the second component of the fluorescence lifetime. However, this scenario is only applicable *in vivo*.

It should be noted that a photoinactivated RC is not equivalent to a closed RC. While both closed RC and photoinactivated RC cannot reduce Q_A , a closed RC has τ_{AV} in the range of ns and remains active. In contrast, a photoinactivated RC is chemically modified (due to photodamage), it is inactive and we have demonstrated that its lifetime becomes shorter, rather than longer as it is seen in the closed RC.

Scenario 4 considers a photoproduct generated under high light that acts as a quencher of PSII fluorescence, which is not related to PSII photodamage. This scenario is a good candidate to explain the fast quenching observed *in vivo* and *in vitro*, as the observed decrease of τ_{AV} is not related to the accumulation of photodamaged PSII. It has been suggested that long-lived quenchers can be formed in LHCII complexes, originating from chlorophyll cations or other radicals produced from chlorophyll triplets³³. As these long-lived quenchers in LHCII are expected to be homogeneously distributed across the PSII population and that LHCII is functionally connected to PSII, they would be able to quench excessive excitations efficiently. Thus, we hypothesize that an unidentified quencher located in the LHCII is a reasonable explanation for the fast quenching component.

Such quencher can be present in leaves and BBY's as both contain functional LHCII. The difference in the lifetime kinetics of shortening of lifetime between the two model systems is due to the difference in the organizational level of both systems (i.e. ability to change stacking or presence of other possible quenchers *in vivo*). This could be the reason why two quenched PSII populations were observed in BBY's.

Since damage to the RC^{3,4} and the repair mechanism¹⁵ is dependent on excitation pressure, the formation of the quenchers before PSII photodamage operates as a pre-emptive photoprotective mechanism that dissipates the accumulated excess energy. This is consistent with the observations that the quencher(s) is (are) accumulated faster (faster shortening of τ_{AV}) than photodamaged PSII (loss of F_V/F_M), thereby slowing down photoinactivation significantly.

The assays to estimate the electron transport rate (ETR) confirmed that PSII was photoinactivated in both model systems. However, the amount of RC damage can only be estimated *in vitro*. RC damage is greater under limited electron transport at the acceptor and donor side, and vice versa, which indicates that RC is susceptible to damage under excessive light excitation. We hypothesize that PSII photodamage is slower than quencher accumulation because the quencher(s) relieve(s) excessive excitation as soon as it is formed.

In summary, the quenchers photoprotect the RC because its photodamage is dependent on excessive excitation and its damage is slower than the loss of the total PSII activity. We hypothesize that the quenching observed in both experimental model systems has the same nature as both models are photodamaged, both models present a quencher that accumulates faster than the photodamaged PSII and the lifetime of both models is shorter than in F_O state. This faster-developing quenching process has two implications: (1) the quencher acts as a "pre-emptive" photoprotection mechanism and (2) quencher formation depends mostly on illumination.

Materials and Methods

Plant material and sample preparation. Fresh and intact spinach leaves were purchased at local markets (during the months of June till August, Wageningen, NL). The leaves were stored at 4 °C in a cold room with the petiole submerged in tap water until use. Only plants with high PSII efficiency, determined by measuring the PSII photochemical yield (F_V/F_M) were selected for all experiments (see chlorophyll (Chl) *a* fluorescence for

PSII efficiency measurements). BBY's were prepared from fresh market spinach as described (see Supplementary Methods).

Photodamage *in vivo*. Before illumination, to inhibit photorepair, leaves were infiltrated with 5 mM lincomycin by passive petiole infiltration for 12 hours in order to ensure its uptake by the leaf tissue^{23,39}. The irradiance at the surface of the leaf during illumination was 1300 $\mu\text{mol photons m}^{-2} \text{s}^{-1}$ of narrow band light ($460 \pm 10 \text{ nm}$ or $660 \pm 10 \text{ nm}$). The sample was illuminated for 30, 60, 120, 180 and 300 min. The control group was kept under identical conditions in darkness inside the photoinhibition boxes (see Supplementary Methods). The experiment was repeated three times.

Photodamage *in vitro*. Samples were illuminated with either 460 or 660 nm light for 1, 2.5, 5, 20 or 60 min ($1300 \mu\text{mol photons m}^{-2} \text{s}^{-1}$). BBY's were then centrifuged at $20,000 \times g$, after which they were re-suspended in standard buffer for cryogenic storage. Aliquots of the sample then were flash frozen in liquid nitrogen and stored at -80°C until use. The experiment was repeated three times.

PSII activity measurements. Leaves were dark adapted for at least 15 min at room temperature. Each leaf was measured from petiole to tip in at three different regions. After the measurements, the leaves were transferred back to the LED photoinhibition boxes. The PSII efficiency was measured at room temperature with an M-PEA fluorometer according to Strasser *et al.*⁴⁰ (Hansatech Instruments). The actinic light intensity was $3000 \text{ photons m}^{-2} \text{s}^{-1}$ for 10 s. All sample manipulation occurred under low light of less than $1 \mu\text{mol photons m}^{-2} \text{s}^{-1}$.

To measure the PSII photochemical efficiency of BBY's, an aliquot of the sample was defrosted at 4°C and then diluted with Buffer A and centrifuged at $20,000 \times g$. Then the concentration of BBY's was adjusted to $150 \mu\text{g}$ of Chl mL^{-1} . PSII efficiency was measured by Chl *a* fluorescence using the same protocol described above. $30 \mu\text{L}$ of the sample was transferred to wet filter paper before measurement.

Colorimetric measurements for BBY's were carried down as reported⁴.

Additional PSII activity measurements were done using P700 oxidation kinetics as 820 nm reflectance changes with the method of⁴¹. P700 signal was recorded simultaneously with the chlorophyll fluorescence using a Multifunctional Plant Efficiency Analyser M-PEA (built by Hansatech Instrument Ltd., King's Lynn, Norfolk, PE30 4NE, UK). The M-PEA sensor unit is designed to detect $820 \pm 25 \text{ nm}$ modulated light from an LED and the detector is shielded with band pass filters at $820 \pm 20 \text{ nm}$.

Time correlated single photon counting (TCSPC). Excitation was carried out by 0.2 ps excitation pulses (412 nm) at a repetition rate of 3.8 MHz. The excitation power was reduced with neutral density filters and the detection rate was kept below $30,000 \text{ photons s}^{-1}$. The diameter of the excitation spot was 2 mm, and the excitation laser power was kept at $1\text{--}5 \mu\text{W}$ to keep PSII RCs (RC) in the open state. The sample was kept in a flow cuvette (flowing speed $\sim 2.5 \text{ mL s}^{-1}$) connected to a sample reservoir (7.5 mL), kept at 20°C . The optical path length of the cuvette was 3 mm and the optical density of the sample was 0.1 per cm. Fluorescence was collected at right angle to the excitation beam, under magic angle (54.7°) polarization with a 680 nm interference filter (15 nm bandwidth), as described previously⁴².

The instrument response function (IRF) was obtained from the 6 ps decay of pinacyanol iodide in methanol⁴³ (the full width at half maximum of the IRF was 35 ps and a resolution of 2 ps per channel was used). Data analysis was performed with a home-built program^{44,45}. For the global analysis the decay lifetime components were kept equal for each run of measurements on the sample exposed to a certain illumination time. The fit quality was judged from the residuals of the fit. Fluorescence decay curves were fitted to a sum of exponentials with the amplitudes a_i and fluorescence decay times τ_i , convoluted with the IRF⁴⁶.

Average lifetimes were calculated as:

$$\tau_{AV} = \sum_{i=1}^N a_i \times \tau_i \quad (1)$$

where $\sum_{i=1}^N a_i = 1$, a_i is the amplitude of the i -th component and τ_i is the lifetime of the i -th component.

Two-photon fluorescence lifetime imaging microscopy (FLIM). Time resolved measurements on leaves were performed on a FLIM setup described⁴⁷. Fluorescence was selected using a 680 nm interference filter (13 nm bandwidth) and a 770 nm cut-off filter was used to prevent detection of the excitation beam. A neutral density filter was used in the excitation path to reduce the excitation light intensity. The output of the detector was coupled to a Becker & Hickl single-photon counting module (SPC 830)⁴⁸. The time window was set to 256 channels and fluorescence was recorded for 5 min at a count rate of 10,000 counts per second. The IRF was obtained from decay of pinacyanol iodide in methanol.

SPCImage software from Becker&Hickl was used to process FLIM images. Fluorescence decay curves were fitted to a sum of N exponentials, convoluted with the IRE, the lifetime components were fitted individually for each pixel. Average lifetimes were calculated using Eq. 1.

Data availability

The datasets generated during and/or analysed during the current study are available in supplementary data and from the corresponding author on reasonable request.

Received: 8 May 2017; Accepted: 21 October 2019;

Published online: 21 November 2019

References

1. Tyystjärvi, E. Photoinhibition of photosystem II and photodamage of the oxygen evolving manganese cluster. *Coord. Chem. Rev.* **252**, 361–376 (2008).
2. Ohad, I., Adir, N., Koike, H., Kyle, D. J. & Inoue, Y. Mechanism of photoinhibition *in vivo*. A reversible light-induced conformational change of reaction center II is related to an irreversible modification of the D1 protein. *J. Biol. Chem.* **265**, 1972–1979 (1990).
3. Zavafer, A., Cheah, M. H., Hillier, W., Chow, W. S. & Takahashi, S. Photodamage to the oxygen evolving complex of photosystem II by visible light. *Sci. Rep.* **5**, 16363, <https://doi.org/10.1038/srep16363> (2015).
4. Ohnishi, N. *et al.* Two-step mechanism of photodamage to photosystem II: step 1 occurs at the oxygen-evolving complex and step 2 occurs at the photochemical reaction center. *Biochemistry* **44**, 8494–8499 (2005).
5. Vass, I. Molecular mechanisms of photodamage in the Photosystem II complex. *BBA-Bioenergetics* **1817**, 209–217 (2012).
6. Vass, I. & Cser, K. Janus-faced charge recombinations in photosystem II photoinhibition. *Trends Plant Sci.* **14**, 200–205, <https://doi.org/10.1016/j.tplants.2009.01.009> (2009).
7. Keren, N., Berg, A., van Kan, P. J., Levanon, H. & Ohad, I. Mechanism of photosystem II photoinactivation and D1 protein degradation at low light: the role of back electron flow. *Proc. Natl. Acad. Sci. USA* **94**, 1579–1584 (1997).
8. Baroli, I. & Melis, A. Photoinhibitory damage is modulated by the rate of photosynthesis and by the photosystem II light-harvesting chlorophyll antenna size. *Planta* **205**, 288–296, <https://doi.org/10.1007/s004250050323> (1998).
9. Behrenfeld, M. J., Prasil, O., Kolber, Z. S., Babin, M. & Falkowski, P. G. Compensatory changes in Photosystem II electron turnover rates protect photosynthesis from photoinhibition. *Photosynth. Res.* **58**, 259–268, <https://doi.org/10.1023/A:1006138630573> (1998).
10. Kato, M. C., Hikosaka, K., Hirotsu, N., Makino, A. & Hirose, T. The excess light energy that is neither utilized in photosynthesis nor dissipated by photoprotective mechanisms determines the rate of photoinactivation in photosystem II. *Plant Cell Physiol.* **44**, 318–325, <https://doi.org/10.1093/pcp/pcg045> (2003).
11. Rehman, A. U., Cser, K., Sass, L. & Vass, I. Characterization of singlet oxygen production and its involvement in photodamage of Photosystem II in the cyanobacterium *Synechocystis* PCC 6803 by histidine-mediated chemical trapping. *BBA-Bioenergetics* **1827**, 689–698, <https://doi.org/10.1016/j.bbabi.2013.02.016> (2013).
12. Hakala, M., Tuominen, I., Keränen, M., Tyystjärvi, T. & Tyystjärvi, E. Evidence for the role of the oxygen-evolving manganese complex in photoinhibition of Photosystem II. *BBA-Bioenergetics* **1706**, 68–80, <https://doi.org/10.1016/j.bbabi.2004.09.001> (2005).
13. Horton, P. & Ruban, A. Molecular design of the photosystem II light-harvesting antenna: photosynthesis and photoprotection. *J. Exp. Bot.* **56**, 365–373, <https://doi.org/10.1093/jxb/eri023> (2005).
14. Ruban, A. V., Johnson, M. P. & Duffy, C. D. P. The photoprotective molecular switch in the photosystem II antenna. *BBA-Bioenergetics* **1817**, 167–181, <https://doi.org/10.1016/j.bbabi.2011.04.007> (2012).
15. Nishiyama, Y., Allakhverdiev, S. I. & Murata, N. A new paradigm for the action of reactive oxygen species in the photoinhibition of photosystem II. *BBA-Bioenergetics* **1757**, 742–749, <https://doi.org/10.1016/j.bbabi.2006.05.013> (2006).
16. Demmig-Adams, B. & Adams, W. W. Photoprotection and Other Responses of Plants to High Light Stress. *Annu. Rev. Plant Phys.* **43**, 599–626, <https://doi.org/10.1146/annurev.pp.43.060192.003123> (1992).
17. Chow, W. S. Photoprotection and photoinhibitory damage. *Adv. Mol. Cell Biol.* **10**, 151–196 (1994).
18. Niyogi, K. K. Photoprotection revisited: Genetic and molecular approaches. *Annu. Rev. Plant Phys.* **50**, 333–359, <https://doi.org/10.1146/annurev.arplant.50.1.333> (1999).
19. Tyystjärvi, E., King, N., Hakala, M. & Aro, E. M. Artificial quenchers of chlorophyll fluorescence do not protect against photoinhibition. *J. Photochem. Photobiol. B.* **48**, 142–147, [https://doi.org/10.1016/S1011-1344\(99\)00022-6](https://doi.org/10.1016/S1011-1344(99)00022-6) (1999).
20. Santabarbara, S., Barbato, R., Zucchelli, G., Garlaschi, F. M. & Jennings, R. C. The quenching of photosystem II fluorescence does not protect the D1 protein against light induced degradation in thylakoids. *FEBS Lett.* **505**, 159–162 (2001).
21. Sarvikas, P., Hakala, M., Pätsikkä, E., Tyystjärvi, T. & Tyystjärvi, E. Action spectrum of photoinhibition in leaves of wild type and npq1-2 and npq4-1 mutants of *Arabidopsis thaliana*. *Plant Cell Physiol.* **47**, 391–400 (2006).
22. Lambrev, P. H., Miloslavina, Y., Jahns, P. & Holzwarth, A. R. On the relationship between non-photochemical quenching and photoprotection of Photosystem II. *BBA-Bioenergetics* **1817**, 760–769 (2012).
23. Matsubara, S. & Chow, W. S. Populations of photo inactivated photosystem II reaction centers characterized by chlorophyll a fluorescence lifetime *in vivo*. *Proc. Natl. Acad. Sci. USA* **101**, 18234–18239, <https://doi.org/10.1073/pnas.0403857102> (2004).
24. Tyystjärvi, E. & Aro, E. M. The rate constant of photoinhibition, measured in lincomycin-treated leaves, is directly proportional to light intensity. *Proc. Natl. Acad. Sci. USA* **93**, 2213–2218 (1996).
25. Jung, J. & Kim, H. S. The Chromophores as Endogenous Sensitizers Involved in the Photogeneration of Singlet Oxygen in Spinach Thylakoids. *Photochem. Photobiol.* **52**, 1003–1009, <https://doi.org/10.1111/j.1751-1097.1990.tb01817.x> (1990).
26. Björkman, O. In *Progress in Photosynthesis Research* 11–18 (Springer, 1987).
27. Holzwarth, A. R., Miloslavina, Y., Nilkens, M. & Jahns, P. Identification of two quenching sites active in the regulation of photosynthetic light-harvesting studied by time-resolved fluorescence. *Chem. Phys. Lett.* **483**, 262–267, <https://doi.org/10.1016/j.cplett.2009.10.085> (2009).
28. Vasil'ev, S. & Bruce, D. Nonphotochemical quenching of excitation energy in photosystem II. A picosecond time-resolved study of the low yield of chlorophyll a fluorescence induced by single-turnover flash in isolated spinach thylakoids. *Biochemistry* **37**, 11046–11054, <https://doi.org/10.1021/bi9806854> (1998).
29. Miloslavina, Y., de Bianchi, S., Dall'Osto, L., Bassi, R. & Holzwarth, A. R. Quenching in *Arabidopsis thaliana* Mutants Lacking Monomeric Antenna Proteins of Photosystem II. *J. Biol. Chem.* **286**, 36830–36840, <https://doi.org/10.1074/jbc.M111.273227> (2011).
30. Gilmore, A. M., Hazlett, T. L. & Debrunner, P. G. & Govindjee. Comparative time-resolved photosystem II chlorophyll a fluorescence analyses reveal distinctive differences between photoinhibitory reaction center damage and xanthophyll cycle-dependent energy dissipation. *Photochem. Photobiol.* **64**, 552–563, <https://doi.org/10.1111/j.1751-1097.1996.tb03105.x> (1996).
31. Iwai, M., Yokono, M., Inada, N. & Minagawa, J. Live-cell imaging of photosystem II antenna dissociation during state transitions. *Proc. Natl. Acad. Sci. USA* **107**, 2337–2342, <https://doi.org/10.1073/pnas.0908808107> (2010).
32. Unlu, C., Drop, B., Croce, R. & van Amerongen, H. State transitions in *Chlamydomonas reinhardtii* strongly modulate the functional size of photosystem II but not of photosystem I. *Proc. Natl. Acad. Sci. USA* **111**, 3460–3465, <https://doi.org/10.1073/pnas.1319164111> (2014).
33. Gruber, J. M. *et al.* Dynamic quenching in single photosystem II supercomplexes. *Phys. Chem. Chem. Phys.* **18**, 25852–25860 (2016).
34. Barzda, V., Vengris, M., Valkunas, L., van Grondelle, R. & van Amerongen, H. Generation of fluorescence quenchers from the triplet states of chlorophylls in the major light-harvesting complex II from green plants. *Biochemistry* **39**, 10468–10477, <https://doi.org/10.1021/bi992826n> (2000).
35. Maxwell, K. & Johnson, G. N. Chlorophyll fluorescence—a practical guide. *J. Exp. Bot.* **51**, 659–668 (2000).
36. Holzwarth, A. R., Miloslavina, Y., Nilkens, M. & Jahns, P. Identification of two quenching sites active in the regulation of photosynthetic light-harvesting studied by time-resolved fluorescence. *Chem. Phys. Lett.* **483**, 262–267 (2009).
37. Demmig-Adams, B. *et al.* Photochemical efficiency of photosystem II, photon yield of O₂ evolution, photosynthetic capacity, and carotenoid composition during the midday depression of net CO₂ uptake in *Arbutus unedo* growing in Portugal. *Planta* **177**, 377–387 (1989).
38. Bilger, W. & Björkman, O. Temperature dependence of violaxanthin de-epoxidation and non-photochemical fluorescence quenching in intact leaves of *Gossypium hirsutum* L. and *Malva parviflora* L. *Planta* **184**, 226–234 (1991).

39. Aro, E. M., McCaffery, S. & Anderson, J. M. Photoinhibition and D1 Protein Degradation in Peas Acclimated to Different Growth Irradiances. *Plant Physiol.* **103**, 835–843 (1993).
40. Strasser, R. J., Tsimilli-Michael, M., Qiang, S. & Goltsev, V. Simultaneous *in vivo* recording of prompt and delayed fluorescence and 820-nm reflection changes during drying and after rehydration of the resurrection plant *Haberlea rhodopensis*. *BBA-Bioenergetics* **1797**, 1313–1326 (2010).
41. Goltsev, V. *et al.* Multifunctional plant efficiency analyzer mPEA used to describe the physiological states of the photosynthetic apparatus. *Agrarni Nauki* **2**, 15–25 (2010).
42. Somsen, O. J. G., Keukens, L. B., de Keijzer, M. N., van Hoek, A. & van Amerongen, H. Structural heterogeneity in DNA: Temperature dependence of 2-aminopurine fluorescence in dinucleotides. *Chemphyschem* **6**, 1622–1627, <https://doi.org/10.1002/cphc.200400648> (2005).
43. van Oort, B. *et al.* Picosecond Fluorescence of Intact and Dissolved PSI-LHCI Crystals. *Biophys J* **95**, 5851–5861, <https://doi.org/10.1529/biophysj.108.140467> (2008).
44. Novikov, E. G., van Hoek, A., Visser, A. J. W. G. & Hofstraat, J. W. Linear algorithms for stretched exponential decay analysis. *Opt. Commun.* **166**, 189–198, [https://doi.org/10.1016/S0030-4018\(99\)00262-X](https://doi.org/10.1016/S0030-4018(99)00262-X) (1999).
45. Digris, A. V. *et al.* Thermal stability of a flavoprotein assessed from associative analysis of polarized time-resolved fluorescence spectroscopy. *Eur. Biophys. J. Biophys.* **28**, 526–531, <https://doi.org/10.1007/s002490050235> (1999).
46. Broess, K., Borst, J. W. & van Amerongen, H. Applying two-photon excitation fluorescence lifetime imaging microscopy to study photosynthesis in plant leaves. *Photosynth. Res.* **100**, 89–96, <https://doi.org/10.1007/s11120-009-9431-5> (2009).
47. Laptinok, S. P. *et al.* Global analysis of Förster resonance energy transfer in live cells measured by fluorescence lifetime imaging microscopy exploiting the rise time of acceptor fluorescence. *Phys. Chem. Chem. Phys.* **12**, 7593–7602 (2010).
48. Becker, W. & Bergmann, A. Lifetime Imaging Techniques for Optical Microscopy. **41** (2003).

Acknowledgements

I.I. This research is financed in part by the BioSolar Cells open innovation consortium, supported by the Dutch Ministry of Economic Affairs, Agriculture and Innovation. A.Z., W.C. and M.C. acknowledges Australian Research Council - Discovery grant DP120100872. A.Z. is grateful to his PhD sponsors National Council of Science and Technology of Mexico (CONACYT), the Mexican Secretariat of Public Education (SEP), the Australian National University and the ARC Centre of Excellence of Translational Photosynthesis. The authors thank Prof. Reto J. Strasser for lending the M-PEA fluorometer used in the present work. A.Z. and I.I. are grateful to Mr. John Philippi for all the technical help during the development of this project. All authors wish to thank Prof. Herbert van Amerongen for his support, insightful discussions and, advice in writing the manuscript.

Author contributions

A.Z. did the experimental design. I.I. and A.Z. performed the experiments and analysis of the data. W.S.C. supervised the project. I.I., A.Z., M.H.C. and W.S.C. participated in the writing of the paper.

Competing interests

The authors declare no competing interests.

Additional information

Supplementary information is available for this paper at <https://doi.org/10.1038/s41598-019-53030-7>.

Correspondence and requests for materials should be addressed to A.Z.

Reprints and permissions information is available at www.nature.com/reprints.

Publisher's note Springer Nature remains neutral with regard to jurisdictional claims in published maps and institutional affiliations.



Open Access This article is licensed under a Creative Commons Attribution 4.0 International License, which permits use, sharing, adaptation, distribution and reproduction in any medium or format, as long as you give appropriate credit to the original author(s) and the source, provide a link to the Creative Commons license, and indicate if changes were made. The images or other third party material in this article are included in the article's Creative Commons license, unless indicated otherwise in a credit line to the material. If material is not included in the article's Creative Commons license and your intended use is not permitted by statutory regulation or exceeds the permitted use, you will need to obtain permission directly from the copyright holder. To view a copy of this license, visit <http://creativecommons.org/licenses/by/4.0/>.

© The Author(s) 2019